

Magnetic composite Hydrodynamic Pump with Laser Induced Graphene Electrodes

Mohammed Asadullah Khan, Ilija R. Hristovski, Member, IEEE, Giovanni Marinaro, and Jürgen Kosel, Senior Member, IEEE

Abstract— A polymer based magneto hydrodynamic pump capable of actuating saline fluids is presented. The benefit of this pumping concept to operate without any moving parts is combined with simple and cheap fabrication methods and a magnetic composite material, enabling a high level of integration. The operating principle, fabrication methodology and flow characteristics of the pump are detailed. The pump electrodes are created by laser printing of polyimide, while the permanent magnet is molded from an NdFeB powder – polydimethylsiloxane (PDMS) composite. The cross-section area of the pump is 240 mm². The electrode length is 5 mm. The magnetic characteristics of the NdFeB-PDMS composite indicate high degree of magnetization, which increases the pump efficiency. Using a saline solution similar to seawater, the pump produces 3.4 mm/s flow velocity at a voltage of 7.5V and a current density of 30 mA/cm².

Index Terms—Magneto hydrodynamics, MHD, NdFeB, PDMS, Magnetic Composite, Laser Printing, Graphene, Polyimide.

I. INTRODUCTION

Micro and mesa scale fluid pumps are an indispensable part of lab on chip systems, where they are used to accomplish a variety of tasks like transport, mixing, segregation, filtration among many others. These pumps can be classified into two categories: (i) Mechanical and (ii) Non-mechanical pumps. In a mechanical pump, structures such as turbines, bellows or diaphragms are utilized to facilitate fluid motion. Magnetic, electrostatic, piezoelectric and thermal actuation can be exploited to drive these structures. Except for turbine based pumps, the flow produced by mechanical pumps is pulsed and thus valves are needed to reduce back-flow. The fabrication of these pumps and the associated valves is complicated and the moving actuators are prone to

This paragraph of the first footnote will contain the date on which you submitted your paper for review. It will also contain support information, including sponsor and financial support acknowledgment. Research reported in this publication was supported by the King Abdullah University of Science and Technology (KAUST).

M. A. Khan, G. Marinaro and J. Kosel are with the Computer, Electrical and Mathematical Sciences and Engineering Division (CEMSE), King Abdullah University of Science and Technology (KAUST), Thuwal 23955-6900, Saudi Arabia (e-mail: mohammedasadullah.khan@kaust.edu.sa; giovanni.marinaro@kaust.edu.sa; jurgen.kosel@kaust.edu.sa).

I.R. Hristovski is with the University of British Columbia, Okanagan campus, Kelowna, British Columbia, Canada V1V 1V7 (e-mail: ilijahri@me.com)

malfunction and can damage sensitive biological specimens [1]. Instead of having moving parts, non-mechanical pumps use physical phenomena such as electrowetting, phase transfer, electrostatics or Lorentz force to induce fluid motion. These are comparatively easy to fabricate and scale better to smaller device dimensions than mechanical pumps [1].

When a current carrying fluid is subjected to a perpendicular magnetic field, the fluid experiences a propelling force orthogonal to both the direction of the current as well as the magnetic field. This force is known as the Lorentz force and the pumps utilizing this propulsion principle are called magneto hydrodynamic (MHD) pumps. Small scale MHD pumps are popular for biofluidic applications [2, 3], while larger MHD pumps have been studied for marine propulsion applications [4, 5]. Unlike electrowetting and electrostatic pumps which require high actuation voltage (>100 V), MHD pumps feature lower operating voltages (generally below 10 V), which mitigates electrostatic discharge problems [1].

MHD pumps are used to pump conductive fluids. Liquid metals such as mercury [6] and gallium have been used as the conductive media for MHD pumps, however they have little practical utility for most applications. To serve practical use cases, it is desirable to utilize ionic fluids such as sea water, urine, blood as the conductive media for a MHD pump. Using a saline fluid for MHD propulsion results in evolution of chlorine gas at the anode, which causes corrosion. In order to avoid corrosion related issues, saline fluid MHD pumps have electrodes fabricated using noble metals such as Gold [2] and Platinum [3]. These materials are very expensive and need complex fabrication techniques to ensure adequate thickness and sidewall coverage. It is quite well-known that graphite electrodes are exceptionally corrosion resistant. In this work, the insulating material polyimide (PI) is converted to conductive graphene by CO₂ laser printing to form the electrodes of the MHD pump [7].

The magnetic field needed for the operation of an MHD pump is typically generated using permanent magnets or coils, which are usually arranged in Helmholtz configuration to provide a uniform magnetic field. For marine propulsion MHD pumps, using superconducting Helmholtz coils is an attractive proposition as very high magnetic field can be produced with relatively low power consumption [4, 5, 8]. In [9], a.c. operation of MHD pump is enabled by driving the coils and the electrodes by synchronous signals, which are always in phase with each other. A.C. operation is attractive as no chlorine gas is evolved, thereby mitigating the corrosion issue. In lab on chip systems, device footprint and power

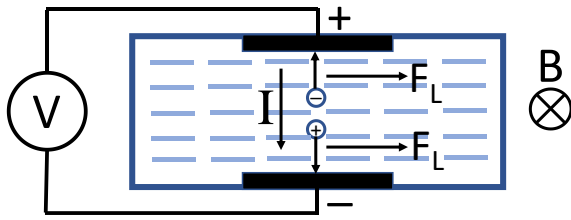


Fig. 1. Schematic and working principle of a typical MHD pump consumption are of prime importance. Coils increase the power consumption of the pump and smaller devices need smaller coils, which provide much less magnetic flux density than miniature permanent magnets, thereby leading to very poor flow rates [9, 10]. Thus, permanent rare earth magnets (NdFeB magnets in particular) are popular in biofluidic MHD pumps [11, 12]. However, these magnets are rigid and cannot be easily integrated with polymer fabrication processes, which are commonly used for lab on chip systems. Polymer composite magnets, on the other hand are flexible, can conform to any arbitrary device shape, provide high magnetic field strength and are processed at lower temperatures, making them easy to integrate within existing fabrication process flows [13]. Although MHD pumps could benefit greatly from the use of polymer composite magnets, they have not been developed yet. In this work, an NdFeB magnetic powder – polydimethylsiloxane (PDMS) composite is utilized as the magnetic field source.

II. WORKING PRINCIPLE

A typical schematic of an MHD pump is depicted in fig. 1. Electrodes are placed along the sidewalls of a fluidic channel, parallel to the direction of the fluid flow. When an electrical field is applied via the electrodes, the cations of the fluid are attracted towards the negative electrode and the anions towards the positive electrode. The motion of the ions constitutes the current, I which flows between the electrodes. A magnetic field with flux density B is applied orthogonal to the direction of the current and the intended fluid flow. An ion moving with a velocity v_i and having a charge q is subject to the Lorentz Force given as

$$\vec{F}_L = q. (\vec{v}_i \times \vec{B}). \quad (1)$$

The anions and cations move in opposite directions and have opposite polarities. Hence, both the cations and the anions experience F_L in the same direction. These ions collide with the adjacent molecules transferring their momentum and causing a net force acting on the liquid in the same direction as F_L . Assuming a rectangular channel of width w , the MHD force is given as

$$F = wIB. \quad (2)$$

If d is the depth of the channel, then the component of pressure acting on the fluid, orthogonal to both the current as well as the magnetic field, is given as

$$p = \frac{IBw}{wd} = \frac{IB}{d}. \quad (3)$$

According to Hagen-Poiseuille law [14], the relationship between pressure, p volumetric flow rate, Q and fluidic resistance, R is

$$p = QR. \quad (4)$$

If L is the length of the rectangular channel and μ is the fluid viscosity, then from [9], fluidic resistance is given by

$$R = \frac{2\mu L(2(w+d))^2}{(wd)^3} = \frac{8\mu L(w+d)^2}{w^3d^3}. \quad (5)$$

Rearranging equation (4) and substituting (3) and (5) in it we have

$$Q = \frac{p}{R} = \frac{IBw^3d^2}{8\mu L(w+d)^2}. \quad (6)$$

If v is the flow velocity, then $Q = vwd$, substituting this in equation (6), we get

$$v = \frac{IBw^2d}{8\mu L(w+d)^2}. \quad (7)$$

Thus, it can be concluded that aside from the channel dimensions and the viscosity of the conductive medium, the flow velocity is directly proportional to the applied current and magnetic flux density.

III. FABRICATION

The fabrication of the MHD pump involves three steps: fabrication of laser induced graphene (LIG) electrodes, fabrication of NdFeB-PDMS composite magnet and final assembly, which are detailed below.

A. Fabrication of LIG Electrodes

A polyamic acid based PI precursor (HD Microsystems PI-2611) is spun coated on a silicon wafer, which has a 2 μm thick thermally grown SiO_2 film on it, at 2000 rpm for 30 sec. It is then baked at 90°C for 90 s, and 150°C for 90s. At a ramp rate of 4°C/min, the substrate is heated to 350°C. It is cured at this temperature for 30 min and gradually cooled down to room temperature. The high temperature curing process is essential to fully imidize the film, orient the polymer and completely dissociate the carrier solvent. Selectively scanning a CO_2 laser with 3 W power and at a speed of 92 mm/s across the PI film transforms it into the LIG electrodes. Unlike the PI film which is an insulator, the LIG electrode has a sheet resistance of 24 Ω/square .

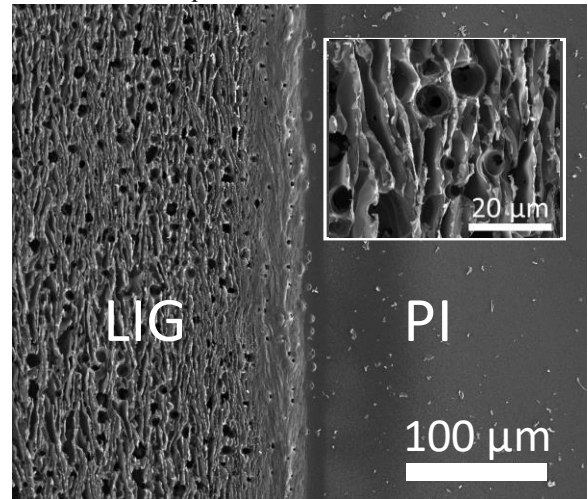


Fig. 2. SEM image depicting the surface morphology of LIG and the PI film, the inset is a zoomed in image of the LIG film highlighting its porous nature

SEM images (fig. 2) reveal that unlike the PI film which is smooth, the LIG electrodes have an uneven highly porous surface. It is theorized that the porous nature of the electrodes is advantageous as it improves the contact area with the saline

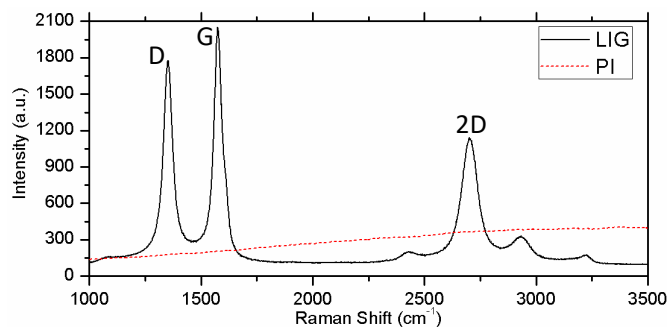
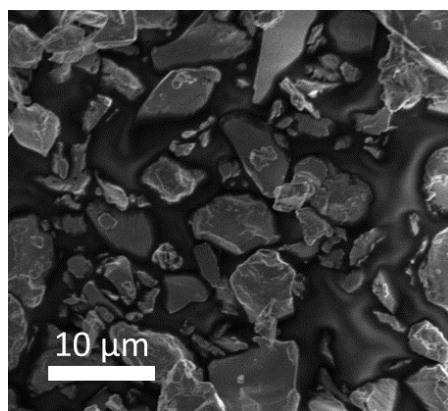
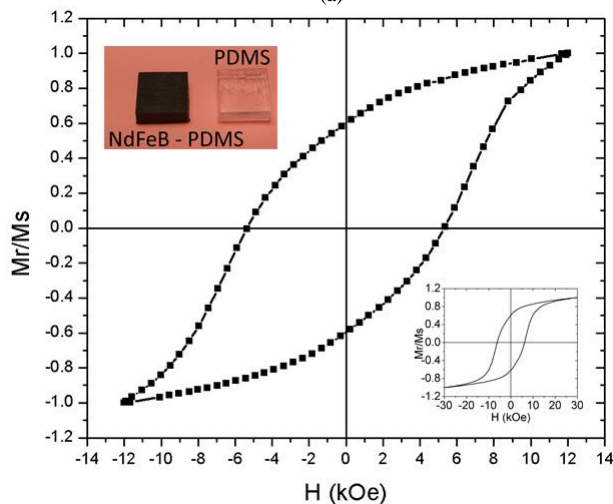


Fig. 3. Raman spectrum of LIG and PI, indicating the D, G and 2D peaks

solution, thereby providing higher current. Raman spectroscopy of the PI and LIG films further reveals the changes produced in the PI film by the laser treatment (fig. 3). The PI film has an unremarkable Raman spectrum, devoid of any prominent features. On the other hand, the LIG Raman spectrum shows 3 prominent peaks. The first peak, which occurs at a shift of $\sim 1350 \text{ cm}^{-1}$ is the D peak, which is attributed to defective and bent sp^2 bonds. The G peak occurs at $\sim 1580 \text{ cm}^{-1}$ and this is due to doubly degenerate zone center E_{2g} mode. Most importantly, a single Lorentzian 2D peak is observed at $\sim 2700 \text{ cm}^{-1}$, which occurs due to second order zone boundary phonons and is indicative of graphene formation. The peak is quite broad, when compared to mono-



(a)



(b)

Fig. 4 (a) SEM image of NdFeB powder and (b) Magnetization curve of NdFeB – PDMS composite. Insets show a block of pure PDMS and a block of NdFeB – PDMS composite as well as the 30 kOe magnetization curve.

layer graphene, which reveals the presence of multiple randomly stacked graphene layers.

B. Fabrication of NdFeB-PDMS composite magnet

PDMS (Dow Corning Corp. Slygard® 184) is prepared by mixing the elastomer and the curing agent in the manufacturer recommended 10:1 weight ratio. NdFeB microparticles (Molycorp MQP-16-7FP, mean particle size $5 \mu\text{m}$) are thoroughly dispersed into the PDMS matrix at 1:1 weight ratio by mechanical stirring. Fig. 4(a) shows an SEM image of the NdFeB particles. This mixture is then poured into a laser patterned poly(methyl methacrylate) mold and subject to vacuum desiccation to eliminate any bubbles. Subsequently, it is cured at 90°C for 60 minutes to form the composite polymer NdFeB magnet. A vibrating sample magnetometer is used to apply a magnetizing field of 1.2 T to the composite magnet, which results in a remanence to saturation magnetization ratio of 0.6, as seen in fig. 4(b). The energy product (BH) value of the composite is 17.1 kJ/m^3 .

C. Final Assembly

A petri dish serves as the MHD pump reservoir. Two pieces of PMMA stuck to the petri dish using an adhesive at a spacing of 1.5 cm serve as the channel sidewalls. The depth of the channel is 1.6 cm. The LIG electrodes are diced, peeled off the substrate wafer and stuck to the PMMA sidewalls using an adhesive tape. The NdFeB-PDMS composite magnet is placed underneath the petri dish to provide the magnetic field necessary for pump operation. The average magnetic field strength in the channel is measured using a Gauss meter and found to be 1.5 mT.

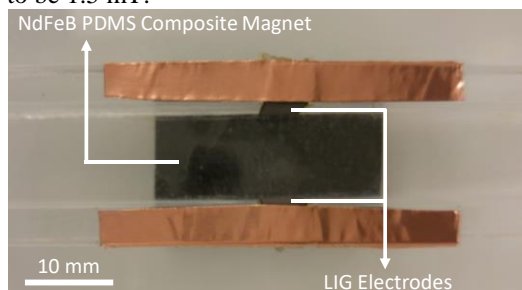


Fig. 5. Photograph of the fabricated MHD pump

IV. RESULTS

The operation of this pump is studied using NaCl solutions with weight concentrations of 2%, 2.5% and 3.0%. At any given concentration, the current increases linearly with the applied voltage (fig. 6(a)). Fitting the obtained data, the slope of the V-I characteristics varies from 254.8Ω for 2% NaCl solution to 172.4Ω for 3% NaCl solution. As expected, the system resistance decreases with increasing salt concentration. In order to study the pumping velocity, hollow glass microspheres (HGMS, diameter $90 - 106 \mu\text{m}$) are introduced into the flow. The voltage is varied from 5 V to 7.5 V and the HGMS motion is captured using an SLR camera with high shutter speed. Since the time between the frames is known, by measuring the distance travelled by the spheres, the velocity of the fluid can be computed.

From equation (7), it is apparent that the flow velocity is

directly proportional to the current and it is expected that the 3% NaCl solution by virtue of its comparatively lower resistance will exhibit best flow velocity. Fig. 6(b) shows the variation of flow velocity with applied voltage for different NaCl concentrations, and in accordance with theory, the 3% NaCl solution tests yield the highest flow rates.

Fig. 6(c) shows flow velocity variation with applied current. This plot includes data obtained at all three concentrations. The data points indicate a linear, directly proportional relationship between the flow velocity and the applied current. Equation (7) is evaluated for the values of current recorded in the experiment and it closely agrees with the experimental data.

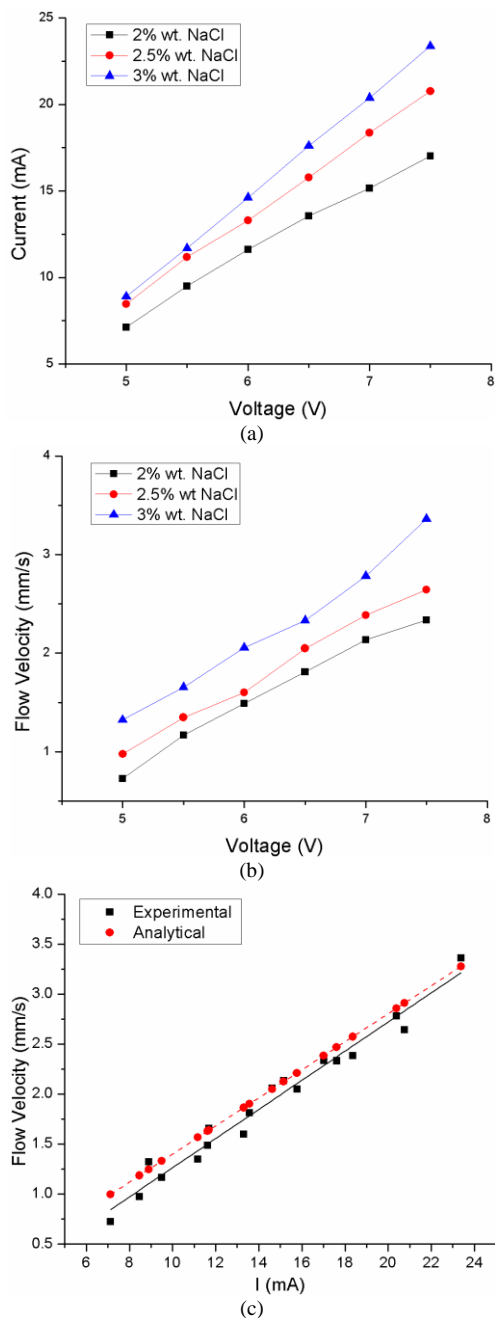


Fig. 6 (a) Variation of current with applied voltage, (b) Change in flow velocity with voltage for 2%, 2.5 % and 3% wt. NaCl saline solutions and (c) Flow variation with current, the analytically computed values match well with the experimental results

V. CONCLUSION

A magnetic composite polymer MHD pump, which can be utilized to actuate ionic liquids is presented in this paper. Instead of using a permanent magnet or coil, a permanently magnetized composite is used as the source of magnetic flux. The composite is magnetized at a field of 1.2 T and the resulting M_r/M_s value of 0.6 indicates that the post cure magnetization process is successful. The electrodes are made up of LIG on polyimide. The Raman spectrum of the LIG electrodes is indicative of the presence of multiple randomly stacked layers of graphene. The porous nature and significant intrinsic conductivity of the LIG electrodes serves the MHD pump well. The MHD device provides a flow velocity proportional to the applied current and pumps a solution similar to sea water (30000 ppm salt concentration by weight) at 0.146 mm/s/mA.

The results show the efficient operation of the MHD pump fabricated with simple fabrication methods and the potential for miniaturization and high integration. The main components of the device are made of flexible material which further provides the means to build mechanically bendable MHD pumps.

REFERENCES

- [1] N. T. Nguyen and X. Huang, "MEMS-micropumps: a review," *Journal of Fluids Engineering-Transactions of the ASME*, 2002.
- [2] C. Das, G. Wang, and F. Payne, "Some practical applications of magnetohydrodynamic pumping," *Sensors and Actuators A: Physical*, vol. 201, pp. 43-48, 2013.
- [3] A. Homay, S. Koster, J. C. T. Eijkel, A. Berg, F. Lucklum, E. Verpoorte, et al., "A high current density DC magnetohydrodynamic (MHD) micropump," *Lab on a Chip*, vol. 5, pp. 466-471, 2005.
- [4] D. L. Mitchell and D. U. Gubser, "Magnetohydrodynamic ship propulsion with superconducting magnets," *Journal of Superconductivity*, vol. 1, pp. 349-364, 1988.
- [5] L. G. Yan, C. W. Sha, K. Zhou, and Y. Peng, "Progress of the MHD ship propulsion project in China," *IEEE Transactions on Applied Superconductivity*, vol. 10, pp. 951-954, March 2000.
- [6] J. Zhong, M. Yi, and H. H. Bau, "Magneto hydrodynamic (MHD) pump fabricated with ceramic tapes," *Sensors and Actuators A: Physical*, vol. 96, pp. 59-66, 2002.
- [7] J. Lin, Z. Peng, Y. Liu, F. Ruiz-Zepeda, and R. Ye, "Laser-induced porous graphene films from commercial polymers," *Nature Communications*, vol. 5, December 2014.
- [8] E. D. Doss and H. K. Geyer, "The need for superconducting magnets for MHD seawater propulsion," in *Proceedings of the 25th Intersociety Energy Conversion Engineering Conference*, 1990, pp. 540-545.
- [9] A. V. Lemoff and A. P. Lee, "An AC magnetohydrodynamic micropump," *Sensors and Actuators B: Chemical*, vol. 63, pp. 178-185, 15 May 2000.
- [10] J. C. T. Eijkel, C. Dalton, C. J. Hayden, and J. P. H. Burt, "A circular ac magnetohydrodynamic micropump for chromatographic applications," *Sensors and Actuators B: Chemical*, vol. 92, pp. 215-221, July 2003.
- [11] L. Huang, W. Wang, M. C. Murphy, and K. Lian, "LIGA fabrication and test of a DC type magnetohydrodynamic (MHD) micropump," *Microsystem Technologies*, vol. 6, pp. 235-240, Nov 2000.
- [12] J. Jang and S. S. Lee, "Theoretical and experimental study of MHD (magnetohydrodynamic) micropump," *Sensors and Actuators A: Physical*, vol. 80, pp. 84-89, March 2000.
- [13] M. A. Khan, A. Alfadhel, and J. Kosel, "Magnetic Nanocomposite Cilia Energy Harvester," *IEEE Transactions on Magnetics*, vol. 52, pp. 1-4, July 2016.
- [14] S. P. Suter and R. Skalak, "The history of Poiseuille's law," *Annual Review of Fluid Mechanics*, vol. 25, pp. 1-20, 1993.